Heliyon 10 (2024) e36585

Contents lists available at ScienceDirect

Heliyon

journal homepage: www.cell.com/heliyon

Research article

miR-155 enhances apoptosis of macrophage through suppressing PI3K-AKT activation in *Pseudomonas aeruginosa* keratitis

Qiang Fu [a,1], Xingyuan Zhu [a,1], Qiongyan Fang [b,1], Hui Han [a], Zhiying Wang [a], Jinye Xie [a], Dong Qian [a], Xinger Wu [a], Yongjian Wu [b], Kang Chen [c,*]

[a] *Zhongshan Cancer Research Institute of Zhongshan City, Zhongshan City People's Hospital, Zhongshan, Guangdong, 528403, China*
[b] *Center for Infection and Immunity, the Fifth Affiliated Hospital of Sun Yat-sen University, Zhuhai, Guangdong Province, 519000, China*
[c] *Department of Laboratory Medicine, Zhongshan City People's Hospital, Zhongshan, Guangdong, 528403, China*

ARTICLE INFO

Keywords:
Pseudomonas aeruginosa
Keratitis
miR-155
Apoptosis
Macrophage

ABSTRACT

Keratitis induced by *Pseudomonas aeruginosa* (*P. aeruginosa*) is an acute and serious corneal inflammation. As a family of gene regulators, miRNAs play a crucial role in modulating host response after microbial invasion. However, their functions in *P. aeruginosa* keratitis remain largely unclear. In the present study, we demonstrated that miR-155 expression was significantly increased in macrophages and corneal tissue after *P. aeruginosa* infection. *In vivo* studies demonstrated that mice with miR-155 knockdown displayed more resistance to *P. aeruginosa* keratitis, with a lower bacterial burden. In addition, *in vitro* and *in vivo* studies indicated that miR-155 enhanced apoptosis of macrophages after *P. aeruginosa* infection, and resulted in a susceptible phenotype of *P. aeruginosa* keratitis. Moreover, miR-155 induced apoptosis through reducing activation of PI3K-Akt signaling pathway. Our data provided evidence of miR-155 mediated apoptosis of macrophage in *P. aeruginosa* keratitis, which may be an underlying target for the therapy of *P. aeruginosa* keratitis and other infectious diseases.

1. Introduction

Pseudomonas aeruginosa (*P. aeruginosa*) is a versatile Gram-negative bacterium that can cause a wide range of infections. As an opportunistic pathogen, it contributes to serious life-threatening infections and increasing mortality in immunocompromised individuals. *P. aeruginosa* infection is the most common cause of bacterial keratitis associated with contact-lens use [1]. *P. aeruginosa* corneal infection (keratitis) is characterized by rapid onset and progression with epithelial defects, underlying stromal infiltration, tissue destruction and corneal ulceration [2]. Strong inflammation and ulceration lead to more severe complications, including anterior chamber hypopyon and descemetocele formation, corneal scarring, and even perforation [3]. Increasing evidence suggest that the severe keratitis caused by *P. aeruginosa* resulted from not only the high-virulence characteristics of the bacteria itself, but also from the excessive host immune inflammatory response [4–6].

The host defense system utilizes a number of strategies to sense and defense against pathogens. However, the immune response to *P. aeruginosa* is not always protective. For instance, macrophages are crucial for bacterial clearance [7]. The role of the macrophage in the host response to *P. aeruginosa* ocular challenge was tested in mice by depletion of macrophages before infection using

* Corresponding author.
E-mail address: ck521620@163.com (K. Chen).
[1] These authors contribute equally to this work.

https://doi.org/10.1016/j.heliyon.2024.e36585
Received 7 September 2023; Received in revised form 15 August 2024; Accepted 19 August 2024
Available online 20 August 2024

subconjunctival injections of liposomes containing [8]. Depletion of macrophages impaired bacterial clearance, increased pro-inflammatory response and promoted neutrophils chemotaxis in the cornea, which resulted in enhanced incidence, severity and chronicity of keratitis [8]. Recently, infection-induced extensive immune cell death including apoptosis, necrosis and pyroptosis, was identify as a major contributor to the overwhelming host immune response in bacterial infectious diseases [9,10]. A large quantity of damage-associated molecular patterns (DAMPs) released from immune cell death could be recognized by pattern recognition receptors (PRRs), such as Toll-like receptors (TLRs), NOD-like receptors, DNA sensors, C-type lectin receptor, and contribute to enhance immune activation [11]. Therefore, strictly control and regulate the extensive immune cell death is beneficial for the bacterial clearance. However, the mechanism of how bacterial infection leads to extensive immune cell death is still not fully understood.

MicroRNAs (miRNAs) have been emerged as important gene regulators of many physiological and pathological processes, including proliferation, apoptosis, differentiation, cell fate determination [12]. Several miRNAs, including miR-155 [13], miR-125b [14], miR-21 [15], miR-146 [16], miR-9 [17], and miR-132 [18] have been identified to be involved in infectious diseases. Their expression could be regulated by various stimuli, such as microbes and inflammatory cytokines (e.g., tumor necrosis factor (TNF)-α, interleukin (IL)-6) [19]. As the first identified inflammatory miRNA, miR-155 is recognized to be an important regulator of inflammation and immune response. miR-155 has been shown to regulate a wide array of genes, including chemokines, cytokines, and transcription factors [20–22]. However, the role of miR-155 in cell death (e.g. apoptosis and necrosis) is intricate. On one hand, miR-155 has been reported to enhanced B-cell immortalization [23], up-regulated breast cancer cell survival [24], induced proliferation and decrease apoptosis of osteosarcoma cells [25]. On the other hand, Levati et al. reported that miR-155 impaired the proliferation and induced the apoptosis of melanoma cells [26]. Likewise, it was also found that miR-155 elevated apoptosis of immune cells such as human dendritic cells (DC) [27] and macrophages [28]. These studies together illustrated that miR-155 had different functions in modulating cell death. However, the role of miR-155 in immune cell death during *P. aeruginosa* keratitis remains unknown.

Our studies revealed that miR-155 expression was up-regulated in macrophages and corneal tissue after *P. aeruginosa* challenge. In addition, mice with miR-155 knockdown displayed a resistant phenotype to *P. aeruginosa* corneal infection, accompanied with reduced pathology score and bacterial burden. Moreover, miR-155 knockdown decreased apoptosis of infiltrated macrophages in corneal tissue as well as macrophage *in vitro* during *P. aeruginosa* challenge. Moreover, miR-155 elevated apoptosis of macrophages by inhibiting the activation of the PI3K/Akt pathway. Collectively, these data demonstrated that miR-155 increased corneal susceptibility by promoting macrophage apoptosis, which may provide potential targets for treatment of *P. aeruginosa* keratitis as well as other infectious diseases.

2. Materials and methods

2.1. Ethics statement

This project has been approved by the Ethics Committee of the Zhongshan City People's Hospital (Zhongshan, China) and in accordance with the Helsinki Declaration (IRB No. 00142).

2.2. Mice and reagents

Eight-week-old C57BL/6 mice were purchased from Jackson laboratory (Bar Harbor, ME). PA strain 19660 and RAW264.7 strain TIB-71 were ordered from the American Type Culture Collection (ATCC). Pseudomonas isolation agar (PIA) (Cat.# BD-292710) was purchased from BD Difco Laboratories (Sparks, MD). miR-155 and control mimic (Cat.# MC13058), LNA-miR-155 inhibitor and LNA-control inhibitor (Cat.# AM13058) were purchased from Applied Biosystems (Foster, CA). DeadEnd™ Fluorometric TUNEL System (Cat.#G3250) was purchased from Promega (Medison, WI). Annexin V-FITC Apoptosis Detection Kit (Cat.# KGA108) was ordered from KeyGEN (Nanjing, China). Protease Inhibitor Cocktail kit (Cat.# 87786) was purchased from Thermo Scientific (Rockford, IL). Quick-start Bradford assay was obtained from Bio-Rad (Hercules, CA). Rabbit anti mouse pAKT antibody (Cat.# ab38449) was purchased from Abcam (Burlingame, CA). Rabbit anti mouse antibodies against Akt (Cat.# 9272), c-Jun N-terminal kinase (JNK) (Cat.# 9252), pJNK (Cat.# 4668), extracellular signal-regulated kinase (ERK) (Cat.# 9102), pERK (Cat.# 4370) and cleaved caspase-3 (Cat.# 9664) were ordered from Cell Signaling Technology (Danvers, MA). Secondary fluorescence Ab (Cat.# 926–68071) was purchased from LI-COR (Lincoln, NE). Phosphatidylinositol-3,4,5-triphosphate (PIP3) (Cat.# P-3900) was obtained from Echelon Biosciences (Salt states, UT). Lipofectamine™ 2000, DMEM medium, FBS, and penicillin-streptomycin were purchased from Life Technologies (Grand Island, NY). Ficoll was ordered from TBDsciences (Shanghai, China). Unless otherwise indicated, all other chemicals were purchased from Sigma-Aldrich (St. Louis, MO, USA). FITC anti-mouse CD45 antibody (Cat.# 157214), APC anti-mouse CD11b antibody (Cat.# 101212), Pacific Blue™ anti-mouse F4/80 antibody (Cat.# 123124) was purchased from Biolegend (California, USA). PE Mouse Anti-Akt (pS473) (Cat.# 561671) and Viability Stain 780 (Cat.# 565388) was purchased from BD biosciences (New Jersey, USA).

2.3. PBMC isolation and macrophage differentiation

Human peripheral blood sample and AB-type serum were obtained from Guangzhou Blood Center (Guangdong, China). The peripheral blood mononuclear cells (PBMCs) were isolated by using Ficoll density gradient centrifugation, seeded (5×10^6 per well) in 24-well plates, cultured in DMEM medium supplemented with 10 % human AB-type serum, and incubated in a standard tissue culture incubator at 37 °C with an atmosphere of 5 % CO_2 and 95 % air. Human monocyte-derived macrophages (MDMs) were prepared as described by others before [29]. Change the medium every three days to remove non-adherent cells, after 9 days, MDMs (>90 %

purity) were used for *in vitro* studies.

2.4. Isolation of peritoneal macrophages

Peritoneal macrophages were isolated from C57BL/6 mice. Briefly, mice were intraperitoneally injected with 1 ml of 3 % Brewer's thioglycollate medium (Difco). After 5 days, peritoneal exudate cells were collected by peritoneal lavage with DMEM, stained with trypan blue, and viable cells (>95 %) were enumerated using a hemocytometer. After a differential cell count, cells were seeded (1×10^6 per well) in 12-well plates and incubated at 37 °C. Non-adherent cells were removed 4 h later and isolated macrophages (>90 % purity) were used for *in vitro* studies.

2.5. Keratitis model and clinical examination

The left cornea of the mice was infected by PA. Briefly, after mice were anesthetized with ethyl ether, the left central cornea was scarified with a 25-gauge needle, and a 5-μL aliquot containing a 1×10^6 CFU/μl of bacterial suspension was applied. LNA-miR-155 inhibitor or LNA-control inhibitor were subconjunctivally injected into the left eye (5 μl/mouse) once a week for three times after ocular infection. Bacterial load was assessed by plate count, as described by previous study [29]. Briefly, corneal tissues were lysed, and bacterial colony-forming units (CFU) were determined by a plate count assay. Corneal disease was graded using an established scale [29]: 0, clear or slight opacity partially or fully covering the pupil; +1, slight opacity partially or fully covering the anterior segment; +2, dense opacity partially or fully covering the pupil; +3, dense opacity covering the entire anterior segment; and +4, corneal perforation or phthisis. Mice were housed in a facility accredited by the American Association of Laboratory Animal Care according to the National Institutes of Health guidelines. Procedures conformed to the Association for Research in Vision and Ophthalmology (ARVO) Resolution on the Use of Animals in Research (https://www.arvo.org/About/policies/statement-for-the-use-of-animals-inophthalmic-and-vision-research/) and were approved by Animal Care Committee of Zhongshan City People's Hospital (Zhongshan, China) (No. K2019-011).

2.6. TUNEL assay and hematoxylin-eosin (H&E) staining

Normal uninfected and infected eyes from C57BL/6 mice (n = 5/group/time) were enucleated at 1 and 5 days postinfection (p.i.). TUNEL staining was performed by using DeadEnd™ Fluorometric TUNEL System according to the manufacturer's instruction. Eyes were fixed in a 3.7 % formaldehyde solution and embedded in paraffin. Four micrometer–thick sections were cut, deparaffinized, rehydrated, and rinsed with DNase-free water. Then, sections were permeabilized using proteinase K solution for 15 min, followed by quenching of endogenous peroxidase with 3 % H_2O_2 in methanol for 5 min. Sections were incubated with 1 × terminal deoxynucleotidyl transferase (TdT enzyme) solution at 37 °C for 1 h to label DNA nick ends, and then treated following the manufacturer's protocol. Control samples were treated similarly but without TdT enzyme treatment.

2.7. RAW264.7 cell culture, transient transfection, and real-time

PCR. RAW 264.7 is a macrophage cell line that was established from a tumor in a male mouse induced with the Abelson murine leukemia virus. RAW264.7 cells were cultured in DMEM medium supplemented with 10 % FBS and 1 % penicillin-streptomycin. Cells were transiently transfected with 30 nM miR-155 or control mimic by using Lipofectamine™ 2000 following the manufacturer's instruction. After 24 h of transfection, cells were washed twice with phosphate buffered saline (PBS) and then challenged with live PA at indicated multiplicity of infection (MOI). Real-time PCR analysis of miR-155 was performed using the TaqMan microRNA Assay kit (Applied Biosystems, Foster City, CA).

2.8. Flow cytometry

The cell staining procedure used in this study was described previously [30]. For macrophage staining, corneal cells were stained with anti-CD45, CD11b, F4/80 mAbs. For phosphorylated AKT staining, corneal cells were treated with the intracellular fixation/permeabilization buffer set (eBioscience, CA, USA) and then stained with AKT mAbs. Flow cytometric analysis was performed on FACS Canto II (BD, NJ, USA), and the data were analyzed using FlowJo software (Tree Star).

2.9. Apoptosis assay

Cell apoptosis was respectively assessed by flow cytometry (FCM) and TUNEL staining. For FCM, phosphatidylserine on the outer cell membrane was measured using an Annexin V-FITC Apoptosis Detection Kit, according to the manufacturer's instruction. In brief, 2×10^5 RAW264.7 cells were treated with miR-155 mimic or LNA-miR-155 inhibitor for 24 h and then infected with PA for 24 h. Cells were washed, resuspended in 500 μl binding buffer, and labeled with 5 μl Annexin V-FITC and 5 μl Propidium Iodide (PI) for 15 min on ice. Then, the labeled cells were analyzed by flow cytometer (Beckman Coulter EPICS XL/MCL, Fullerton, CA). For TUNEL staining, DNA strand breaks were assessed with a DeadEnd™ Fluorometric TUNEL System. In brief, 2×10^5 RAW264.7 cells treated with above procedure were fixed in cold paraformaldehyde, washed with PBS, and permeabilized overnight in cold 0.2 % Trition®X-100 in PBS. After incubation with 1 × balance buffer, slices were incubated with 1 × TdT enzyme solution at 37 °C in a humidity chamber for 1 h to

label the DNA nick ends, and then the reaction was stopped with 2 × saline-sodium citrate buffer. Control cell slices were treated similarly but without TdT enzyme. Slices were photographed under a microscope (Axiophot; Carl Zeiss, Oberkochen, Germany) with digital imagery (Axiocam; Carl Zeiss).

2.10. RT-qPCR

Reverse transcription was performed using a PrimeScript RT Reagent Kit (Cat.# RR037A, Takara). The expression levels of human or mouse miRNA-155 was measured using hsa-miR-155 (Cat.# 002287) or mmu-miR-155 (Cat.# 002571) from TaqMan MicroRNA Assays (ThermoFisher). The relative expression level of microRNAs was normalized by U6 (Cat.# 001973, Applied Biosystems).

2.11. Western blotting

Cells were washed twice with ice-cold PBS and lysed with lysis buffer containing 1 % (v/v) protease inhibitor cocktail, 1 mM phenylmethylsulfonyl fluoride, and 1 mM DL-Dithiothreitol (DTT). The protein concentration in cell lysates was determined by Quick-start Bradford assay. Cell lysates with equivalent protein amounts (20 μg) were loaded, separated by 12 % SDS-PAGE, and then transferred to a supported NC membrane. After blockage, blots were incubated with primary Ab overnight, followed by secondary fluorescence Ab for 1 h, and detected using LI-COR ODY-2391 (Lincoln, NE) following the manufacturer's protocol.

2.12. Statistical analysis

Two-tailed Student's *t*-test was used to analyze the data of real-time RT-PCR and apoptosis assay. Data were represented as the mean ± SEM (n = 5) and considered statistically significant at $p < 0.05$.

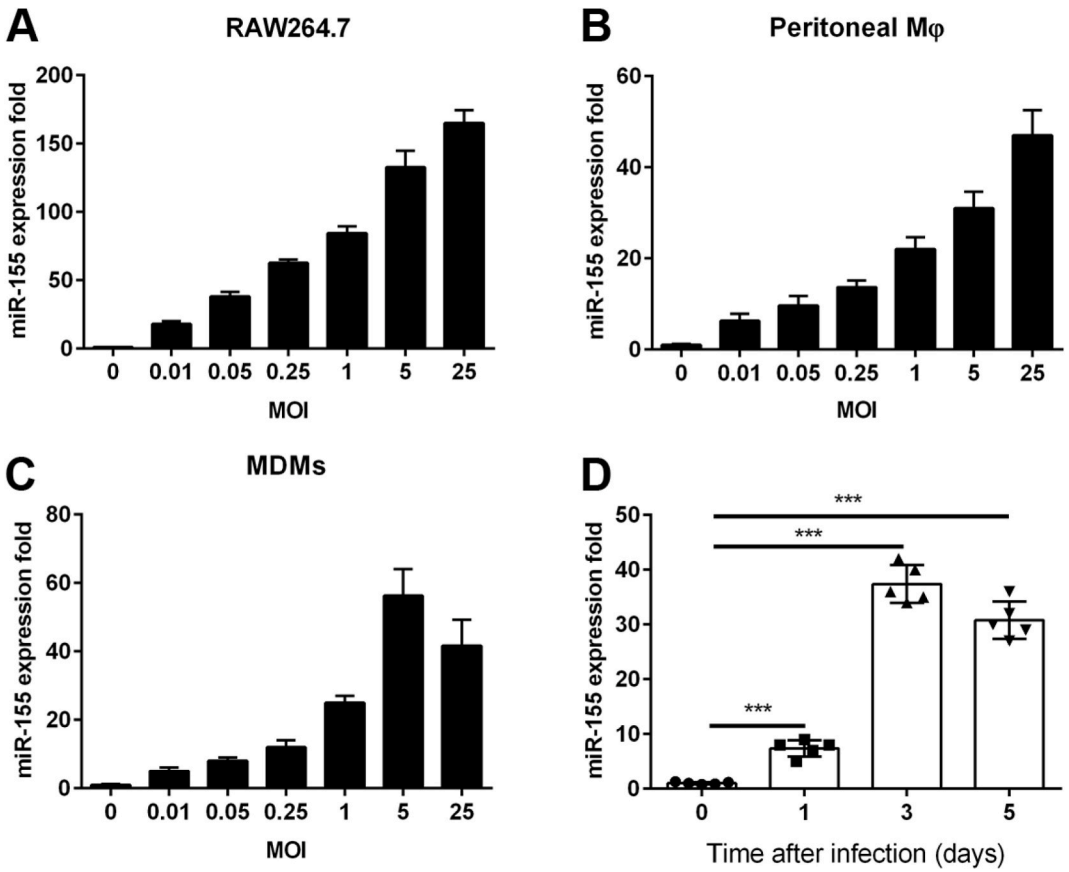

Fig. 1. miR-155 expression was up-regulated in different macrophages and corneal tissue by *P. aeruginosa* infection. (A–C) miR-155 expression levels were measured by real-time PCR after *P. aeruginosa* challenge at indicated MOI in (A) macrophage-like RAW264.7 cells, (B) murine peritoneal macrophages, and (C) human monocyte-derived macrophages. (D) miR-155 expression in normal and *P. aeruginosa* infected mouse corneas 1, 3, and 5 days after infection. Data are mean ± SEM with 5 mice/time points.

3. Results

3.1. miR-155 expression was up-regulated in P. aeruginosa infected macrophage and keratitis

As an important immune-regulatory microRNA, miR-155 plays a significant role in antimicrobial immune responses. To detect whether miR-155 expression is induced by *P. aeruginosa* infection, we tested the expression levels of miR-155 by RT-PCR in different types of macrophages after *P. aeruginosa* challenge, including macrophage-like RAW264.7 cells (Fig. 1A), murine peritoneal macrophages (Fig. 1B), and human monocyte-derived macrophages (MDMs) (Fig. 1C). The results showed that miR-155 expression was significantly up-regulated in all three types of macrophages after *P. aeruginosa* challenge in a dose-dependent manner. Next, we generated the experimental murine model of *P. aeruginosa* keratitis according to our previous study [31], and then tested the expression of miR-155 expression in corneal tissue. The results showed that miR-155 expression was significantly enhanced in mouse corneas 1, 3, and 5 days after infection (Fig. 1D), which is consistent with the macrophage data.

3.2. miR-155 contributes to corneal susceptibility to P. aeruginosa infection

To investigate whether miR-155 participates in *P. aeruginosa* keratitis, mice with subconjunctival injection of LNA-miR-155

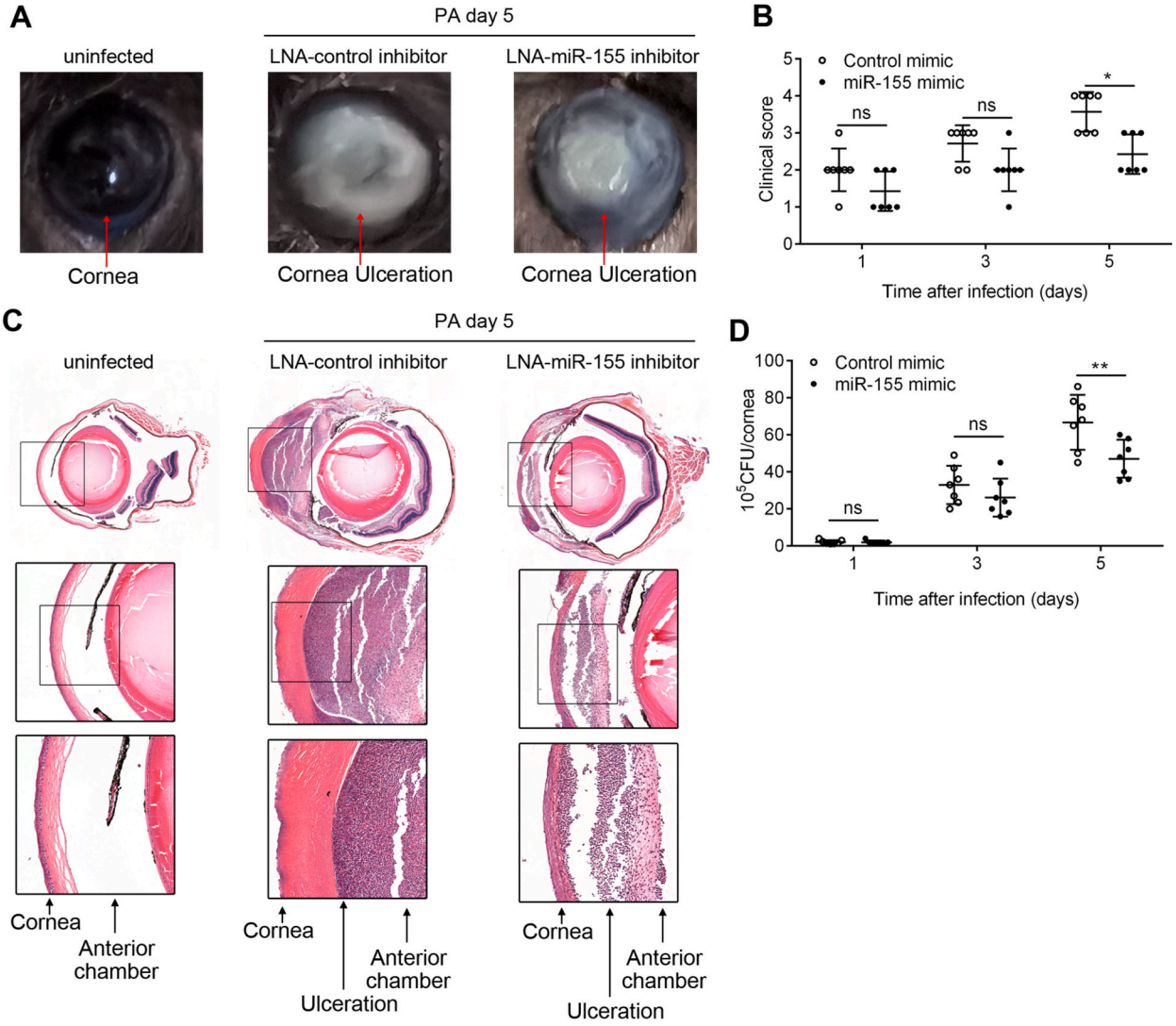

Fig. 2. miR-155 knockdown mice are resistant to *P. aeruginosa* corneal infection. (A) Representative photographs of infected eyes in LNA-control inhibitor or LNA-miR-155 inhibitor treated mice were taken 5 days after *P. aeruginosa* (PA) infection. (**B**) Clinical score was recorded for each mouse 1, 3, and 5 days after infection. (**C**) H&E staining of mouse eye section. (**D**) Bacterial load in the infected cornea was examined by plate count 5 days after infection.

inhibitor or LNA-control inhibitor were infected with *P. aeruginosa*. miR-155 knockdown (with LNA-miR-155 inhibitor) mice displayed a highly resistant phenotype against *P. aeruginosa* ocular infection, compared with control mice (Fig. 2A and B). Representative photographs of corneas 5 day after infection are provided in Fig. 2A. The result showed that the miR-155 knockdown mice displayed

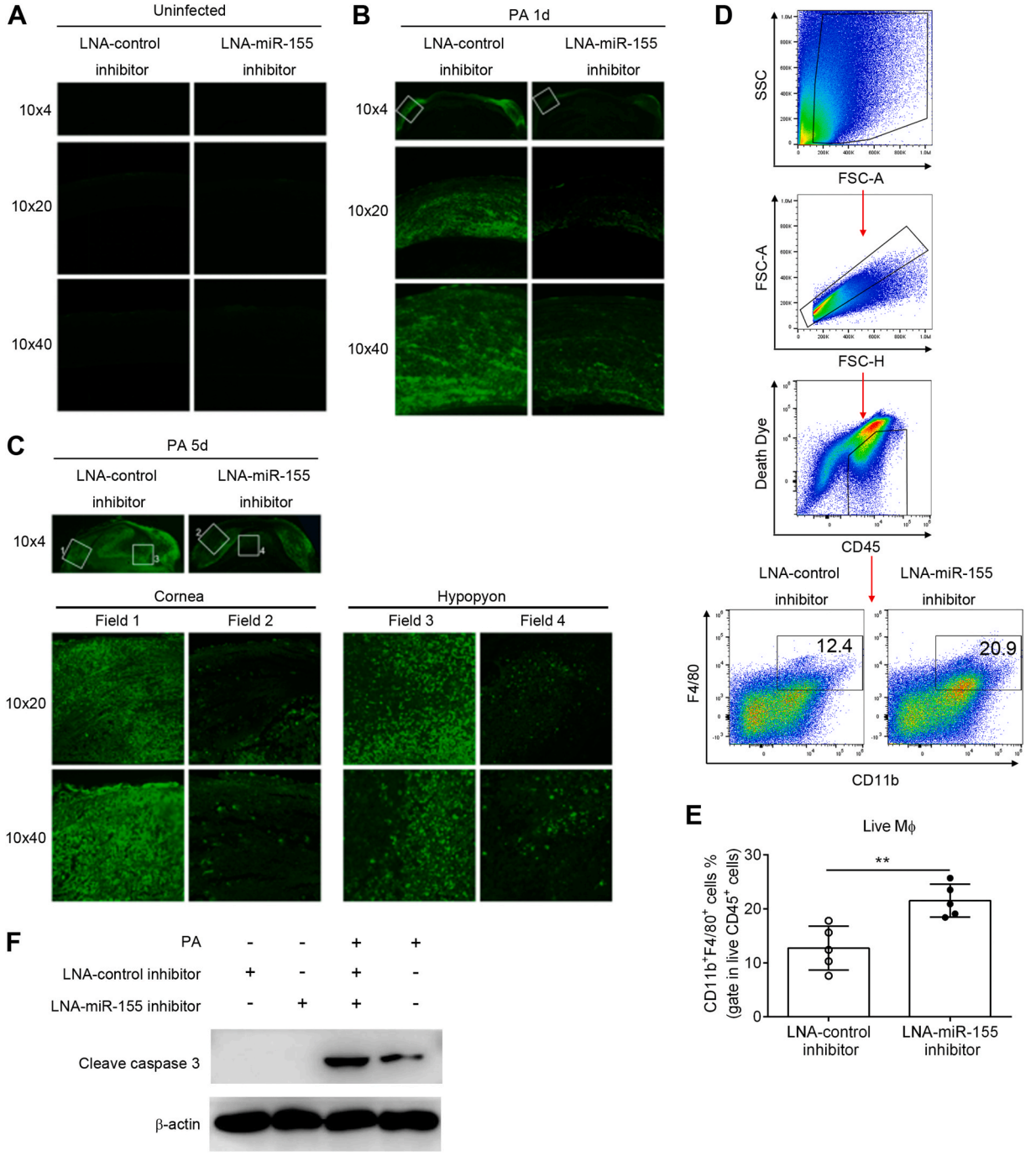

Fig. 3. miR-155 knockdown decreased *P. aeruginosa* infection induced macrophage quantity in corneas. (A–C) TUNEL staining was detected in corneas of LNA-control inhibitor or LNA-miR-155 inhibitor treated mice at 1, 5 day postinfection of PA. (C) TUNEL staining was detected in both corneas and hypopyon of LNA-miR-155 inhibitor or LNA-control inhibitor treated mice at 5 day postinfection of PA. Images shown are representative of three individual experiments (n = 5 mice/group/each experiment). (D, E) Live macrophages were detected by flow cytometry in corneas of LNA-control inhibitor or LNA-miR-155 inhibitor treated mice at 5 day postinfection of PA. Cells were gated as single, live (death dye $^{-}$) CD45^{+} cells. Corneal macrophages were gated as CD11b^{+}F4/80^{+} cells. (F) The expressions of cleaved caspase-3 were determined by Western blot in corneas of LNA-control inhibitor or LNA-miR-155 inhibitor treated mice at 1 day postinfection of PA.

decreased clinical score at 5 day after infection (Fig. 2B). By 5 days after infection, miR-155 knockdown mice displayed less severe corneal disease (clinical score, +3/+4), whereas corneas from control mice were perforated (clinical score, +2/+3) (Fig. 2B). Moreover, H&E staining showed that miR-155 knockdown mice had less severe pathology in the corneal tissues than control mice (Fig. 2C). We next assessed the effect of miR-155 on the bacterial component of disease pathogenesis, using a plate count assay. A reduced bacterial load was detected in the infected corneas of miR-155 knockdown mice, compared with control mice, 5 days after infection, whereas no difference between these 2 groups was detected 1 and 3 days after infection (Fig. 2D). These data suggested that

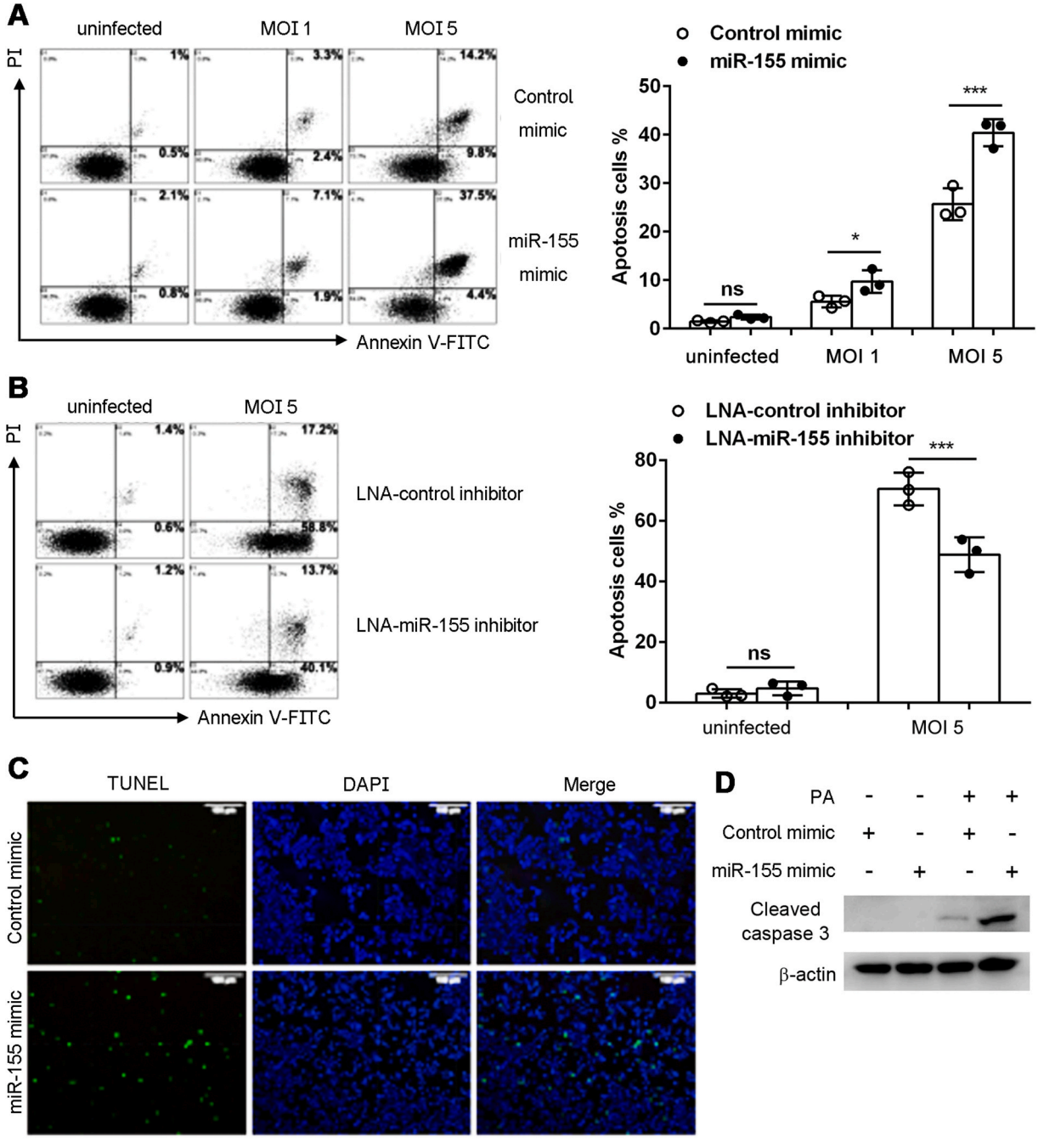

Fig. 4. miR-155 elevated macrophage apoptosis after *P. aeruginosa* infection. RAW264.7 cell apoptosis levels were determined after treatment with miR-155 mimic or LNA-miR-155 inhibitor for 24 h and then stimulation with PA for 24 h. Cell apoptosis was detected using Annexin V-FITC/PI analysis apoptosis kit by flow cytometry (A, B), and TUNEL staining (C) under the Fluorescence microscope. The apoptotic cells were stained in green. (D) RAW264.7 cells were treated with miR-155 mimic or control mimic for 24 h and then stimulation with PA for 24 h. The expressions of cleaved caspase-3 were determined by Western blot.

miR-155 promotes host susceptibility to *P. aeruginosa* infection.

3.3. miR-155 knockdown mice displayed more apoptosis than control mice in the P. aeruginosa-infected corneas

Next, apoptosis in corneas at 1 and 5 days post infection was examined by TUNEL staining. Apoptotic cells increased in control corneas at 1 day post infection. While less apoptotic cells were found in miR-155 knockdown (with LNA-miR-155 inhibitor) corneas

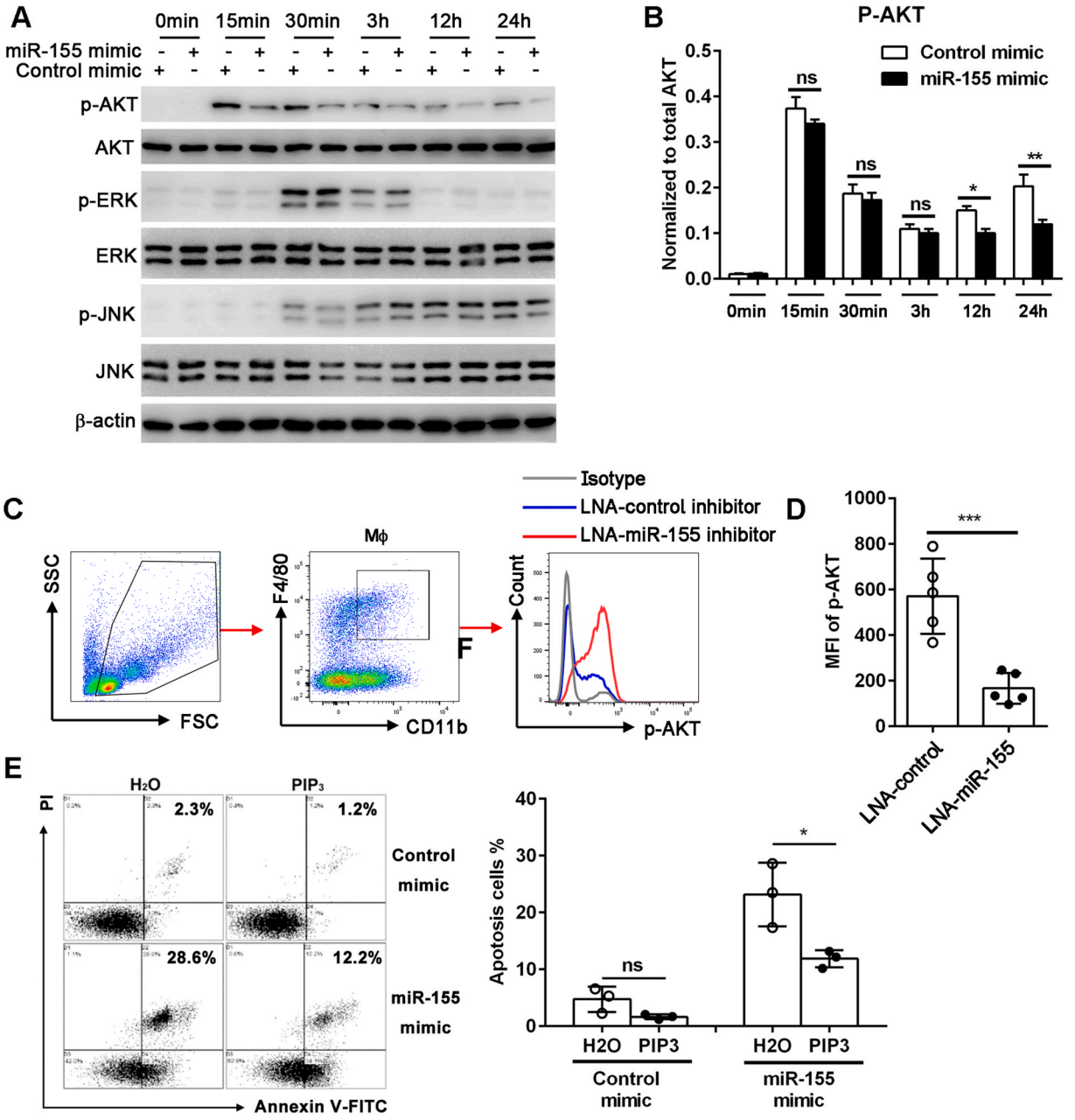

Fig. 5. PIP3-mediated Akt activation involved in miR-155 elevated macrophage apoptosis during *P. aeruginosa* infection. (A, B) RAW264.7 cells were transfected with miR-155 mimic vs control mimic for 24 h. Then protein levels of total and phosphorylated Akt, ERK, and JNK after PA stimulation at different time points (0min, 15min, 30min, 3 h, 12 h, 24 h) were detected by western blotting. Data represent three individual experiments. (C, D) Phosphorylated Akt in macrophages were detected by flow cytometry in corneas of LNA-control inhibitor or LNA-miR-155 inhibitor treated mice at 5 day postinfection of PA. Corneal macrophages were gated as $CD11b^{+}F4/80^{+}$ cells. Phosphorylated Akt levels were analyzed in corneal macrophages. (E, F) RAW264.7 cells were transfected with miR-155 mimic for 24 h, treated with PIP3 for 4 h, and then challenged with PA at MOI 5. Cell apoptosis/necrosis was examined by FCM with Annexin V and PI staining. Data represent three individual experiments.

(Fig. 3A and B). At 5 days post infection, although a larger amount of TUNEL-positive cells were detected in corneas and hypopyon from either miR-155 knockdown or control mice, miR-155 knockdown mice displayed less intense TUNEL-positive cells than did the control mice (Fig. 3C). These results indicated that miR-155 enhanced apoptosis of infiltrated inflammatory cells in *P. aeruginosa* keratitis. To analyze whether miR-155 affected macrophage quantity, we determined the frequency of live infiltrating macrophage in the corneas of *P. aeruginosa* keratitis with flow cytometry (Fig. 3D). The results showed that the frequency of live $CD11b^{+}F4/80^{+}$macrophage was increased in the corneal tissue of miR-155 knockdown mice (Fig. 3E). Moreover, miR-155 knockdown inhibited the expression of cleaved caspase-3 in corneal tissue (Fig. 3F). These data indicated that miR-155 promote apoptosis in the *P. aeruginosa*-infected corneas.

3.4. miR-155 promoted macrophage apoptosis upon P. aeruginosa infection

To further determine the role of miR-155 on macrophage apoptosis, RAW264.7 cells were transfected with miR-155 mimic or LNA-miR-155 inhibitor, and stimulated with *P. aeruginosa* at indicated MOI for 24 h. Apoptosis levels were examined by flow cytometry and TUNEL staining. When compared to uninfected cells, *P. aeruginosa* infection increased the percentages of apoptotic cells, and miR-155 overexpression gradually and significantly enhanced the apoptosis of RAW264.7 cells (Fig. 4A). Moreover, LNA-miR-155 inhibitor reduced the percentages of apoptotic cells compared with the LNA-control treated (Fig. 4B). In addition, the results of TUNEL staining showed that more TUNEL positive cells were detected in the miR-155 overexpressed RAW264.7 cells compared with the control (Fig. 4C). Furthermore, miR-155 overexpression promoted the expression of cleaved caspase-3 in RAW264.7 cells (Fig. 4D). These data together indicated that *P. aeruginosa* challenge induced macrophage apoptosis in a dose-dependent manner and miR-155 further enhanced the *P. aeruginosa*-induced macrophage apoptosis.

3.5. miR-155 inhibited activation of Akt signal pathway in macrophages after P. aeruginosa infection

To investigate the mechanism of miR-155-mediated induction of macrophage apoptosis, protein levels of total and phosphorylated Akt, ERK, and JNK were tested by western blotting in miR-155 overexpressed vs control mimic treated RAW264.7 cells after *P. aeruginosa* infection. The results showed that phosphorylated Akt levels were significantly inhibited by overexpression of miR-155 after *P. aeruginosa* infection in each time point (5min, 30min, 3 h, 12 h, 24 h), whereas the levels of phosphorylated ERK and JNK were comparable between miR-155 overexpressed and control group (Fig. 5A and B). To further confirm the role of miR-155 on Akt signal pathway *in vivo*, we determined the phosphorylated Akt in macrophage of corneal tissue with flow cytometry. The results showed that phosphorylated Akt levels were significantly reduced in macrophage of miR-155 knockdown corneal tissue after *P. aeruginosa* infection (Fig. 5C and D). To confirm whether miR-155 enhanced the *P. aeruginosa*-induced apoptosis of macrophages through inhibiting Akt activation, RAW264.7 cells were sequentially transfected with miR-155 mimic, treated with PIP3 (an activator of Akt), and then challenged with *P. aeruginosa*. Results shown that the percentages of apoptotic cells were reduced after PIP3 treatment, demonstrating PIP3 reversed the miR-155-promoted apoptosis of macrophages (Fig. 5E and F). These data indicated that Akt signal pathway may be involved in miR-155-mediated macrophage apoptosis after *P. aeruginosa* challenge.

4. Discussion

As an immune regulator, miR-155 is highly conserved in many species, broadly expressed in various organs, tissues, and cells, and plays an important role in antimicrobial immune responses [32,33]. In the present study, we examined the expression of miR-155 in *P. aeruginosa*-challenged macrophages, and explored the role of miR-155 in modulating apoptosis of macrophage during *P. aeruginosa* keratitis.

Previous studies have demonstrated that miR-155 expression was up-regulated in macrophages infected with *Porphyromonas gingivalis* [34], *Francisella tularensis* [35], *Brucella* [36], vesicular stomatitis virus [37], Epstein-Barr virus [23], and herpes simplex virus [38]. Our *in vitro* data also showed that miR-155 was significantly up-regulated in different types of macrophages after *P. aeruginosa* infection, in a dose-dependent manner suggesting the potential role of miR-155 in *P. aeruginosa* infection. The function of miR-155 in cell death is complicated [39,40]. Results from treatment with either miR-155 mimic or LNA inhibitor showed that miR-155 enhanced macrophages apoptosis after *P. aeruginosa* infection. *P. aeruginosa* infection induced apoptotic cells and miR-155 knockdown with LNA inhibitor attenuated the apoptosis of macrophages after *P. aeruginosa* keratitis *in vivo*. More importantly, corneal staining displayed most of the apoptotic cells (as detected by positive TUNEL staining) were located either in the cornea stroma or anterior chamber, implying that the majority of infiltrated inflammatory cells in the cornea stroma or anterior chamber were at the stage of apoptosis. These findings indicated that miR-155 involved in immune cell death-related signaling pathways which are activated by *P. aeruginosa* infection.

Phosphoinositide 3-kinases (PI3K) can phosphoryle phosphatidylinositol (PtdIns) at its 3′, 4′ and 5’ hydroxyl sites, and the phosphorylated product is named PtdIns-3-4-5-P3 (PIP3) [41]. PIP3 is abundant in the plasma membrane of cells as a critical second messenger in the process of cell growth, proliferation, and survival [42]. This messenger interacts with the proteins containing PIP3-binding domains such as pleckstrin homology (PH) domain [43]. Akt, the serine/threonine kinase with PH domain, is the major molecule which can be activated by PIP3 [44]. PI3K-Akt signaling pathway plays a critical role in the regulation of cell death, survival and proliferation [45,46]. For instance, the activation of PI3K-Akt pathway promoted phosphorylation of BAD to block BAD-induced cell death, therefore increased cell survival [47]. Moreover, phosphorylated Akt inhibited caspase-9, which is an important molecule of apoptosis signaling cascade, and thus repressed cell death [48]. Mechanical experiments shown that phosphorylated Akt levels were

significantly decreased in miR-155 overexpression macrophages after PA challenge, and PIP3 reversed the miR-155-promoted apoptosis in *P. aeruginosa* stimulated macrophages [49]. Therefore, miR-155 may enhance *P. aeruginosa*-induced apoptosis of macrophages through inhibiting the activation of PI3K-Akt pathway, which was consistent with previous studies [49]. However, these findings seemed contradictive to the previous report, which demonstrated that miR-155 repressed expression of SHIP-1 (a negative regulator of Akt), and thereby improved PI3K-Akt activation [20]. The underlying mechanism needs further investigation.

Mitogen-activated protein kinases (MAPKs) such as ERK, JNK, and p38, have shown to regulate miR-155 expression in different ways. For example, Yin et al. reported that the activation of B-cell receptor induced miR-155 expression through ERK and JNK pathways rather than p38 pathway [50]. Rahadiani et al. found that the miR-155 expression was induced by latent membrane protein-1 (LMP-1) of EB virus primarily through p38 and NF-κB pathways [51]. In the present study, the phosphorylation of ERK and JNK were comparable between miR-155 overexpressed and control groups, suggesting that ERK and JNK were not involved in the miR-155 mediated apoptosis of macrophages in *P. aeruginosa* infection.

Macrophage bacterial clearance is critical to host defense against bacterial infection. For example, alveolar macrophages sensed, chemotaxed, and, with high efficiency, phagocytosed inhaled bacterial pathogens such as *P. aeruginosa* and *S. aureus* [52]. Some miRNAs (such as miR-9, miR-125b, miR-132) participate in regulating the activation and bactericidal activity of macrophage [53]. In the present study, *in vivo* data indicated that miR-155 contribute to the corneal susceptibility in response to *P. aeruginosa* infection, as shown by less pathology and increased bacterial burden in miR-155 knockdown corneas compared with WT mice. Therefore, we hypothesized that miR-155 may accelerate the disease progression of *P. aeruginosa* keratitis by enhancing apoptosis of macrophage, which resulted in impairing bacterial clearance.

On the other side, multiple studies have reported the role of macrophages cell death in microbial infections, although the conclusions were still intricate. Zhou et al. found that *P. aeruginosa* susceptible C57BL/6 mice displayed more severe disease (corneal perforation) with a delayed apoptosis compared with resistant BALB/c mice, indicating that the immune cell apoptosis was protective against *P. aeruginosa* infection and keratitis [54]. Moreover, pathogen induced cell lysis or release of pathogen-filled apoptotic bodies would be rapidly taken up by other immune cells in the infection niche. The large quantity of DAMPs released from immune cell death could be recognized by PRRs, such as TLRs [55], and contribute to enhance inflammation. Persistent inflammatory cells recruitment and the consistent excessive inflammation contribute to the severity of *P. aeruginosa* keratitis.

In conclusion, our study demonstrated that the expression of miR-155 was significantly enhanced in macrophages after *P. aeruginosa* infection. Furthermore, miR-155 enhanced macrophage apoptosis after *P. aeruginosa* infection through suppressing the activation of PI3K-Akt signaling pathway, thus contributed to a susceptible phenotype of *P. aeruginosa* keratitis. These data provided new evidence of miR-155-mediated apoptosis in macrophage, which may be a potential target for treatment of *P. aeruginosa* keratitis and other infectious diseases.

5. Conclusion

Our study highlights the importance of the miR-155 in the susceptible phenotype of *P. aeruginosa* keratitis. These findings provide insights into the pathogenesis of *P. aeruginosa* keratitis and offer potential strategies for the clinical translation, which may help develop new therapeutic interventions for *P. aeruginosa* keratitis with clinical complications.

Funding statement

This work was supported by grants National Natural Science Foundation of China (31670880, 81401645, and 81401058); Science and Technology Program of Guangdong (2015B090903063, 2014A020212641, and 2016A020215142); Zhongshan Science and Technology Foundation (2017B1009 and 2016B1001); and Guangdong Medical Science and Technology Research funding project (A2016097).

Data availability statement

Data included in article/supp. material/referenced in article.

Additional information

No additional information is available for this paper.

CRediT authorship contribution statement

Qiang Fu: Writing – original draft, Investigation, Funding acquisition. **Xingyuan Zhu:** Formal analysis, Data curation. **Qiongyan Fang:** Resources, Methodology. **Hui Han:** Methodology. **Zhiying Wang:** Data curation. **Jinye Xie:** Methodology. **Dong Qian:** Formal analysis. **Xinger Wu:** Supervision. **Yongjian Wu:** Writing – review & editing. **Kang Chen:** Methodology, Investigation, Funding acquisition, Formal analysis, Data curation, Conceptualization.

Declaration of competing interest

The authors declare that they have no known competing financial interests or personal relationships that could have appeared to influence the work reported in this paper.

Appendix A. Supplementary data

Supplementary data related to this article can be found at https://doi.org/10.1016/j.heliyon.2024.e36585.

References

[1] J.H. Mah-Sadorra, et al., Trends in contact lens-related corneal ulcers, Cornea 24 (1) (2005) 51–58.
[2] L.D. Hazlett, Corneal response to Pseudomonas aeruginosa infection, Prog. Retin. Eye Res. 23 (1) (2004) 1–30.
[3] S. Lakhundi, R. Siddiqui, N.A. Khan, Pathogenesis of microbial keratitis, Microb. Pathog. 104 (2017) 97–109.
[4] B. Wonnenberg, et al., The role of IL-1beta in Pseudomonas aeruginosa in lung infection, Cell Tissue Res. 364 (2) (2016) 225–229.
[5] L. Wolf, et al., IL-17A-mediated expression of epithelial IL-17C promotes inflammation during acute Pseudomonas aeruginosa pneumonia, Am. J. Physiol. Lung Cell Mol. Physiol. 311 (5) (2016) L1015–L1022.
[6] N. Gao, et al., Opposing effects of IL-1Ra and IL-36Ra on innate immune response to Pseudomonas aeruginosa infection in C57bl/6 mouse corneas, J. Immunol. 201 (2) (2018) 688–699.
[7] L. Chen, et al., Inflammatory responses and inflammation-associated diseases in organs, Oncotarget 9 (6) (2018) 7204–7218.
[8] S.A. McClellan, et al., Macrophages restrict Pseudomonas aeruginosa growth, regulate polymorphonuclear neutrophil influx, and balance pro- and anti-inflammatory cytokines in BALB/c mice, J. Immunol. 170 (10) (2003) 5219–5227.
[9] Z. Cheng, et al., The critical roles and mechanisms of immune cell death in sepsis, Front. Immunol. 11 (2020) 1918.
[10] T. Bergsbaken, S.L. Fink, B.T. Cookson, Pyroptosis: host cell death and inflammation, Nat. Rev. Microbiol. 7 (2) (2009) 99–109.
[11] O. Takeuchi, S. Akira, Pattern recognition receptors and inflammation, Cell 140 (6) (2010) 805–820.
[12] D.P. Bartel, MicroRNAs: target recognition and regulatory functions, Cell 136 (2) (2009) 215–233.
[13] P.S. Eis, et al., Accumulation of miR-155 and BIC RNA in human B cell lymphomas, Proc. Natl. Acad. Sci. U.S.A. 102 (10) (2005) 3627–3632.
[14] E. Tili, et al., Modulation of miR-155 and miR-125b levels following lipopolysaccharide/TNF-alpha stimulation and their possible roles in regulating the response to endotoxin shock, J. Immunol. 179 (8) (2007) 5082–5089.
[15] S.R. Case, et al., MicroRNA-21 inhibits toll-like receptor 2 agonist-induced lung inflammation in mice, Exp. Lung Res. 37 (8) (2011) 500–508.
[16] K.D. Taganov, et al., NF-kappaB-dependent induction of microRNA miR-146, an inhibitor targeted to signaling proteins of innate immune responses, Proc. Natl. Acad. Sci. U.S.A. 103 (33) (2006) 12481–12486.
[17] F. Bazzoni, et al., Induction and regulatory function of miR-9 in human monocytes and neutrophils exposed to proinflammatory signals, Proc. Natl. Acad. Sci. U. S.A. 106 (13) (2009) 5282–5287.
[18] S. Mulik, et al., Role of miR-132 in angiogenesis after ocular infection with herpes simplex virus, Am. J. Pathol. 181 (2) (2012) 525–534.
[19] M.P. Gantier, New perspectives in MicroRNA regulation of innate immunity, J. Interferon Cytokine Res. 30 (5) (2010) 283–289.
[20] R.M. O'Connell, et al., Inositol phosphatase SHIP1 is a primary target of miR-155, Proc. Natl. Acad. Sci. U.S.A. 106 (17) (2009) 7113–7118.
[21] A. Androulidaki, et al., The kinase Akt1 controls macrophage response to lipopolysaccharide by regulating microRNAs, Immunity 31 (2) (2009) 220–231.
[22] A.L. Cardoso, et al., miR-155 modulates microglia-mediated immune response by down-regulating SOCS-1 and promoting cytokine and nitric oxide production, Immunology 135 (1) (2012) 73–88.
[23] S.D. Linnstaedt, et al., Virally induced cellular microRNA miR-155 plays a key role in B-cell immortalization by Epstein-Barr virus, J. Virol. 84 (22) (2010) 11670–11678.
[24] W. Kong, et al., MicroRNA-155 regulates cell survival, growth, and chemosensitivity by targeting FOXO3a in breast cancer, J. Biol. Chem. 285 (23) (2010) 17869–17879.
[25] S. Bhattacharya, et al., Increased miR-155-5p and reduced miR-148a-3p contribute to the suppression of osteosarcoma cell death, Oncogene 35 (40) (2016) 5282–5294.
[26] L. Levati, et al., MicroRNA-155 targets the SKI gene in human melanoma cell lines, Pigment Cell Melanoma Res 24 (3) (2011) 538–550.
[27] C. Lu, et al., miR-221 and miR-155 regulate human dendritic cell development, apoptosis, and IL-12 production through targeting of p27kip1, KPC1, and SOCS-1, Blood 117 (16) (2011) 4293–4303.
[28] D.S. Ghorpade, et al., MicroRNA-155 is required for Mycobacterium bovis BCG-mediated apoptosis of macrophages, Mol. Cell Biol. 32 (12) (2012) 2239–2253.
[29] K. Chen, et al., beta-Catenin promotes host resistance against Pseudomonas aeruginosa keratitis, J. Infect. 67 (6) (2013) 584–594.
[30] K. Chen, et al., Stimulator of interferon genes promotes host resistance against Pseudomonas aeruginosa keratitis, Front. Immunol. 9 (2018) 1225.
[31] K. Yang, et al., miR-155 suppresses bacterial clearance in Pseudomonas aeruginosa-induced keratitis by targeting Rheb, J. Infect. Dis. 210 (1) (2014) 89–98.
[32] A. Rodriguez, et al., Requirement of bic/microRNA-155 for normal immune function, Science 316 (5824) (2007) 608–611.
[33] I. Faraoni, et al., miR-155 gene: a typical multifunctional microRNA, Biochim. Biophys. Acta 1792 (6) (2009) 497–505.
[34] C. Li, et al., miR-155 promotes macrophage pyroptosis induced by Porphyromonas gingivalis through regulating the NLRP3 inflammasome, Oral Dis. 25 (8) (2019) 2030–2039.
[35] T.J. Cremer, et al., MiR-155 induction by F. novicida but not the virulent F. tularensis results in SHIP down-regulation and enhanced pro-inflammatory cytokine response, PLoS One 4 (12) (2009) e8508.
[36] X. Zhang, et al., MicroRNA-155 expression with Brucella infection in vitro and in vivo and decreased serum levels of MicroRNA-155 in patients with brucellosis, Sci. Rep. 12 (1) (2022) 4181.
[37] P. Wang, et al., Inducible microRNA-155 feedback promotes type I IFN signaling in antiviral innate immunity by targeting suppressor of cytokine signaling 1, J. Immunol. 185 (10) (2010) 6226–6233.
[38] S. Bhela, et al., Role of miR-155 in the pathogenesis of herpetic stromal keratitis, Am. J. Pathol. 185 (4) (2015) 1073–1084.
[39] Y.T. Ro, et al., Salmonella-induced miR-155 enhances necroptotic death in macrophage cells via targeting RIP1/3, Mol. Med. Rep. 18 (6) (2018) 5133–5140.
[40] J. Liu, et al., MicroRNA-155 prevents necrotic cell death in human cardiomyocyte progenitor cells via targeting RIP1, J. Cell Mol. Med. 15 (7) (2011) 1474–1482.
[41] J.A. Engelman, J. Luo, L.C. Cantley, The evolution of phosphatidylinositol 3-kinases as regulators of growth and metabolism, Nat. Rev. Genet. 7 (8) (2006) 606–619.
[42] L.E. Rameh, L.C. Cantley, The role of phosphoinositide 3-kinase lipid products in cell function, J. Biol. Chem. 274 (13) (1999) 8347–8350.
[43] T.G. Kutateladze, Translation of the phosphoinositide code by PI effectors, Nat. Chem. Biol. 6 (7) (2010) 507–513.
[44] D.P. Brazil, Z.Z. Yang, B.A. Hemmings, Advances in protein kinase B signalling: AKTion on multiple fronts, Trends Biochem. Sci. 29 (5) (2004) 233–242.
[45] B.D. Manning, A. Toker, AKT/PKB signaling: navigating the network, Cell 169 (3) (2017) 381–405.

[46] C.R. McNamara, A. Degterev, Small-molecule inhibitors of the PI3K signaling network, Future Med. Chem. 3 (5) (2011) 549–565.
[47] S.R. Datta, et al., Akt phosphorylation of BAD couples survival signals to the cell-intrinsic death machinery, Cell 91 (2) (1997) 231–241.
[48] M.H. Cardone, et al., Regulation of cell death protease caspase-9 by phosphorylation, Science 282 (5392) (1998) 1318–1321.
[49] Z. Fan, et al., MiR-155 promotes interleukin-1beta-induced chondrocyte apoptosis and catabolic activity by targeting PIK3R1-mediated PI3K/Akt pathway, J. Cell Mol. Med. 24 (15) (2020) 8441–8451.
[50] Q. Yin, et al., B-cell receptor activation induces BIC/miR-155 expression through a conserved AP-1 element, J. Biol. Chem. 283 (5) (2008) 2654–2662.
[51] N. Rahadiani, et al., Latent membrane protein-1 of Epstein-Barr virus induces the expression of B-cell integration cluster, a precursor form of microRNA-155, in B lymphoma cell lines, Biochem. Biophys. Res. Commun. 377 (2) (2008) 579–583.
[52] A.S. Neupane, et al., Patrolling alveolar macrophages conceal bacteria from the immune system to maintain homeostasis, Cell 183 (1) (2020) 110–125 e11.
[53] S. Roy, miRNA in macrophage development and function, Antioxidants Redox Signal. 25 (15) (2016) 795–804.
[54] Z. Zhou, et al., Substance P delays apoptosis, enhancing keratitis after Pseudomonas aeruginosa infection, Invest. Ophthalmol. Vis. Sci. 49 (10) (2008) 4458–4467.
[55] E. Venereau, C. Ceriotti, M.E. Bianchi, DAMPs from cell death to new life, Front. Immunol. 6 (2015) 422.